ELSEVIER

Ore Geology Reviews 10 (1996) 231–250

ORE GEOLOGY REVIEWS

Pyrite composition and ore genesis in the Prince Lyell copper deposit, Mt Lyell mineral field, western Tasmania, Australia

Oliver L. Raymond

Australian Geological Survey Organisation, GPO Box 378, Canberra, ACT, 2601, Australia

Received 26 October 1994; accepted 22 May 1995

Abstract

The Prince Lyell copper–gold–silver deposit occurs in the late Cambrian Mt Read Volcanics, at Queenstown, Tasmania. Steeply plunging, broadly conformable lenses of disseminated and stringer pyrite–chalcopyrite mineralisation occur in quartz–sericite–chlorite rocks derived from intense alteration of predominantly felsic lavas and volcaniclastic rocks. Middle Devonian deformation has substantially modified primary sulphide textures.

Although extensively fractured, pyrite grains in the ore have retained their original pre-deformation internal structure and chemistry which are revealed by etching and electron microprobe analysis. Earliest sulphide mineralisation produced oscillatory zoned, cobalt-rich pyrite (Pyrite I), coeval with chalcopyrite mineralisation. Cobalt-rich pyrite is commonly associated with Cambrian volcanic rocks in western Tasmania and suggests a volcanogenic origin for the ore fluids at Prince Lyell. Pyrite I was corroded by later hydrothermal fluids and reprecipitated as unzoned, trace element-poor pyrite (Pyrite II), commonly as overgrowths on Pyrite I cores. Minor amounts of a second cobalt-rich pyrite (Pyrite III) occurs with Pyrite II in composite pyrite overgrowths. Sulphur isotope ratios from all pyrite generations fall within a small range (3 to 11‰). In situ isotopic analyses showed no consistent $\delta^{34}S$ variation between the various pyrite generations, suggesting recycling of sulphur derived from a single Cambrian volcanogenic source.

Hematite alteration, derived from oxidised fluids possibly from the adjacent hematitic Owen Conglomerate, occurs in the structural footwall volcanics and the Great Lyell fault zone. Hematite inclusions in Pyrite II and III indicate that these pyrite generations occurred after or during deposition of the conglomerate. It is postulated that Pyrite II and III were deposited during waning volcanism, contemporaneous with Owen Conglomerate sedimentation in the late Cambrian or early Ordovician. The Great Lyell fault would have acted as a growth fault margin between a terrestrial basin, filling rapidly from the east, and the volcanic terrane to the west. The scenario raises the possibility that the concentration of mineral deposits and hematitic alteration along the Great Lyell fault resulted from the subsurface interaction of reduced volcanogenic fluids and oxidised basin waters along the growth fault contact.

1. Introduction

The Mount Lyell mining field at Queenstown on the west coast of Tasmania has supported continuous mining for over a century. Seventeen significant mineral deposits have been discovered on the field. Early mining was centred on the high grade copper deposits in the North Lyell area and on The Blow deposit. Subsequently, the majority of ore from the Mount Lyell field was extracted from the West Lyell

SSDI 0169-1368(95)00025-9

area, comprising the Prince Lyell, "A" Lens and Royal Tharsis copper orebodies. More than 110 Mt of ore at an average grade of 1.8% Cu, 3.0 g/t Ag and 0.6 g/t Au had been mined from the field to June 1993.

This study arose from an investigation of the more recently exposed, southern parts of the Prince Lyell orebody below 14 Level or zero RL (approximately 250 metres below the original open cut). Microtextural and geochemical examination of pyrite mineralisation by etching and electron microprobe analysis have provided some constraints on mineral paragenesis and fluid composition not previously recognised.

2. Geological setting

The Mt Lyell mineral field occurs within the Central Volcanic Complex of the Mt Read Volcanics, an arcuate belt of middle Cambrian (503 Ma; Perkins and Walshe, 1993), calc-alkaline volcanics which host a number of polymetallic volcanic hosted massive sulphide (VMS) deposits including Rosebery, Hercules, Que River and Hellyer (Fig. 1). The Mount Read Volcanics are interpreted to have been erupted in an extensional regime onto ophiolitic rocks previously obducted over continental crust (Berry and Crawford, 1988). Solomon and Groves (1994) suggested that the volcanics formed in a back-arc basin well to the west of the site of subduction following plate collision, while sedimentation took place in the Dundas Trough to the west. The predominantly rhyolitic–dacitic rocks of the Central Volcanic Complex at Mt Lyell are faulted against the late Cambrian–early Ordovician siliciclastic Owen Conglomerate on the east along the Great Lyell fault (Fig. 2). The overlying Pioneer Beds and Gordon Limestone are locally unconformable on the Owen Conglomerate along the Haulage Unconformity, reflecting slumping or drag folds in the Owen Conglomerate adjacent to the Great Lyell growth fault (Solomon, 1967; Berry, 1990b), or perhaps an early Ordovician phase of deformation (Arnold and Carswell, 1990).

The Mt Lyell rocks were deformed during the middle Devonian Tabberabberan orogeny, so that the Prince Lyell orebody occurs within the steeply west-dipping, overturned limb of a large D_1 anticline (Cox, 1981). The D_1 cleavage (S_1) is not preserved in the altered volcanic rocks, but is in the Owen Conglomerate. A later phase of generally N–S compression (D_2) produced WNW-trending folds and faults. During this phase, a fault-bounded zone through the Mt Lyell area known as the Linda Disturbance deformed D_1 structures and the Great Lyell fault, and a regionally penetrative upright cleavage was imposed throughout the altered volcanics (S_2). This foliation in the Prince Lyell area dips steeply to the southwest, parallel to the regional volcanic layering and to the orientation of the Prince Lyell copper mineralisation (Fig. 3). The strong down-dip continuity of the orebody is parallel to an L_2 mineral lineation. Major discrete faults or shears through the Prince Lyell sequence are rare as most of the strain has been accommodated by movement along the S_2 cleavage. Metamorphic conditions during the Devonian did not exceed lower greenschist facies (Cox, 1981).

Volcanics which conformably and disconformably overlie and underlie the altered mine sequence volcanics (Cox, 1981) are not hydrothermally altered, illustrating the grossly strata-bound nature of the zone of alteration (Walshe and Solomon, 1981). Four main types of sulphide mineral deposits are recognised in the Mount Lyell field (Walshe and Solomon, 1981):

1. disseminated and stringer pyrite–chalcopyrite (e.g., Prince Lyell, A lens, Royal Tharsis, Western Tharsis),
2. bornite–chalcopyrite (e.g., North Lyell, 12 West),
3. massive pyrite–chalcopyrite (e.g., The Blow),
4. massive stratiform pyrite–galena–sphalerite–chalcopyrite (e.g., Tasman, Comstock open cut).

Several small deposits containing native copper and cuprite, derived from leaching or erosion of Cambrian sulphides, occur within clay-rich horizons of the Ordovician Gordon Limestone (Markham, 1968; Solomon, 1969). Although largely recrystallised, the massive sulphide ores (types 3 and 4, above) preserve some laminated and colloform textures, suggesting a possible sea-floor exhalative origin. The larger but lower grade disseminated pyrite–chalcopyrite deposits (type 1) are generally found stratigraphically beneath the massive sulphide deposits and the bornite–chalcopyrite ores.

3. Theories of ore genesis

The evolution of ore genesis theories at Mount Lyell is summarised in Fig. 4. Earliest workers on the Mt Lyell field considered the mineralisation to be of epigenetic replacement origin, with fluids focussed along the Great Lyell Fault at its intersection with the Linda Disturbance during Devonian tectonic activity (e.g., Gregory, 1905; Hills, 1927; Nye et al., 1934). Hall and Solomon (1962) first suggested a genetic link between the mineralisation and the Cambrian host volcanics, proposing that Devonian fluids may have derived ore components from an earlier Cambrian mineralisation.

By the 1970's to early 1980's, prevailing thought favoured a Cambrian volcanogenic origin for the Mount Lyell orebodies. Petrographic studies recognised the deformation of original sulphide textures, limiting the age of mineralisation to pre-D_2 deformation (e.g., Markham, 1968; Cox, 1981). Recent stud-

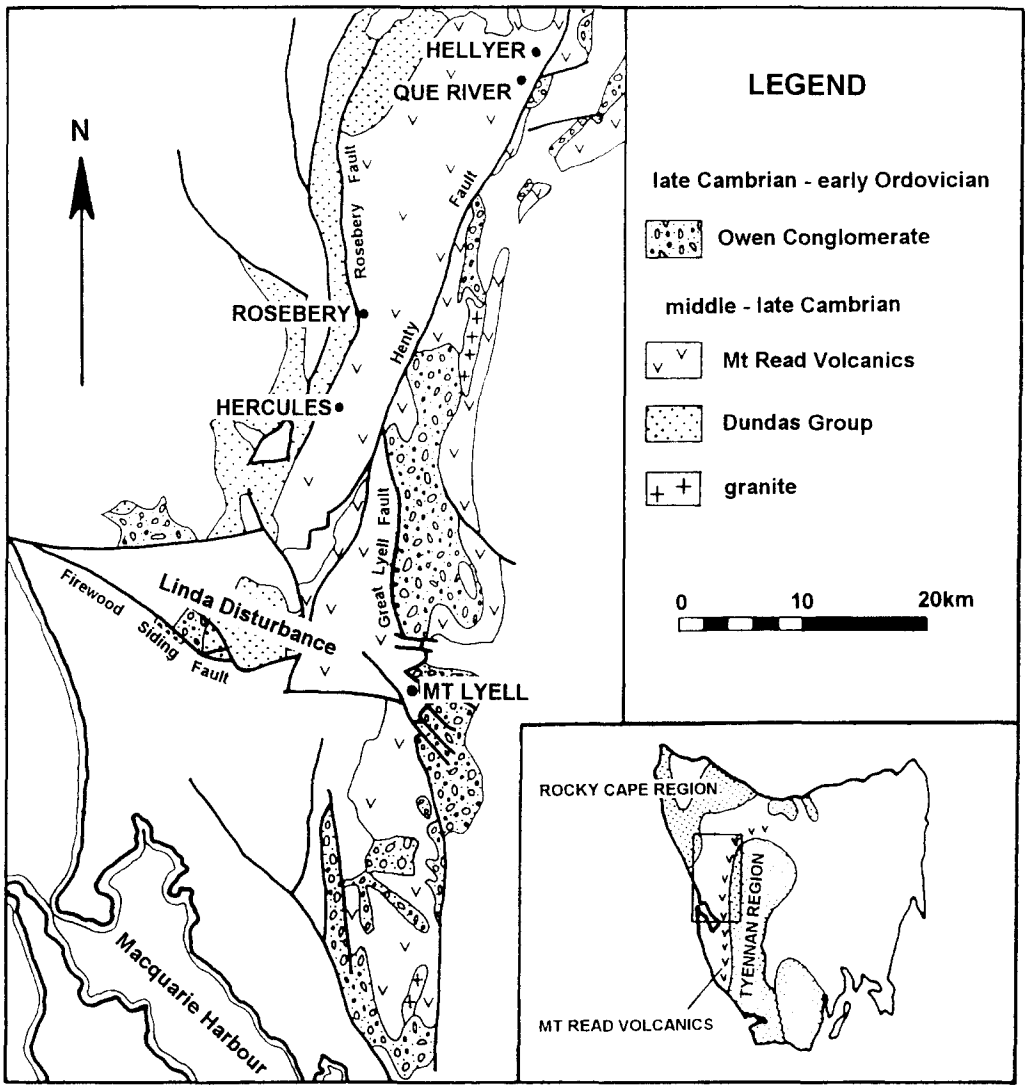

Fig. 1. Geological sketch map of the middle Cambrian to early Ordovician rocks of western Tasmania and major ore deposits of the Mt Read Volcanics. Inset shows the location of the Mt Read belt relative to Tasmanian Precambrian regions (shaded) (modified after Corbett and Solomon, 1989).

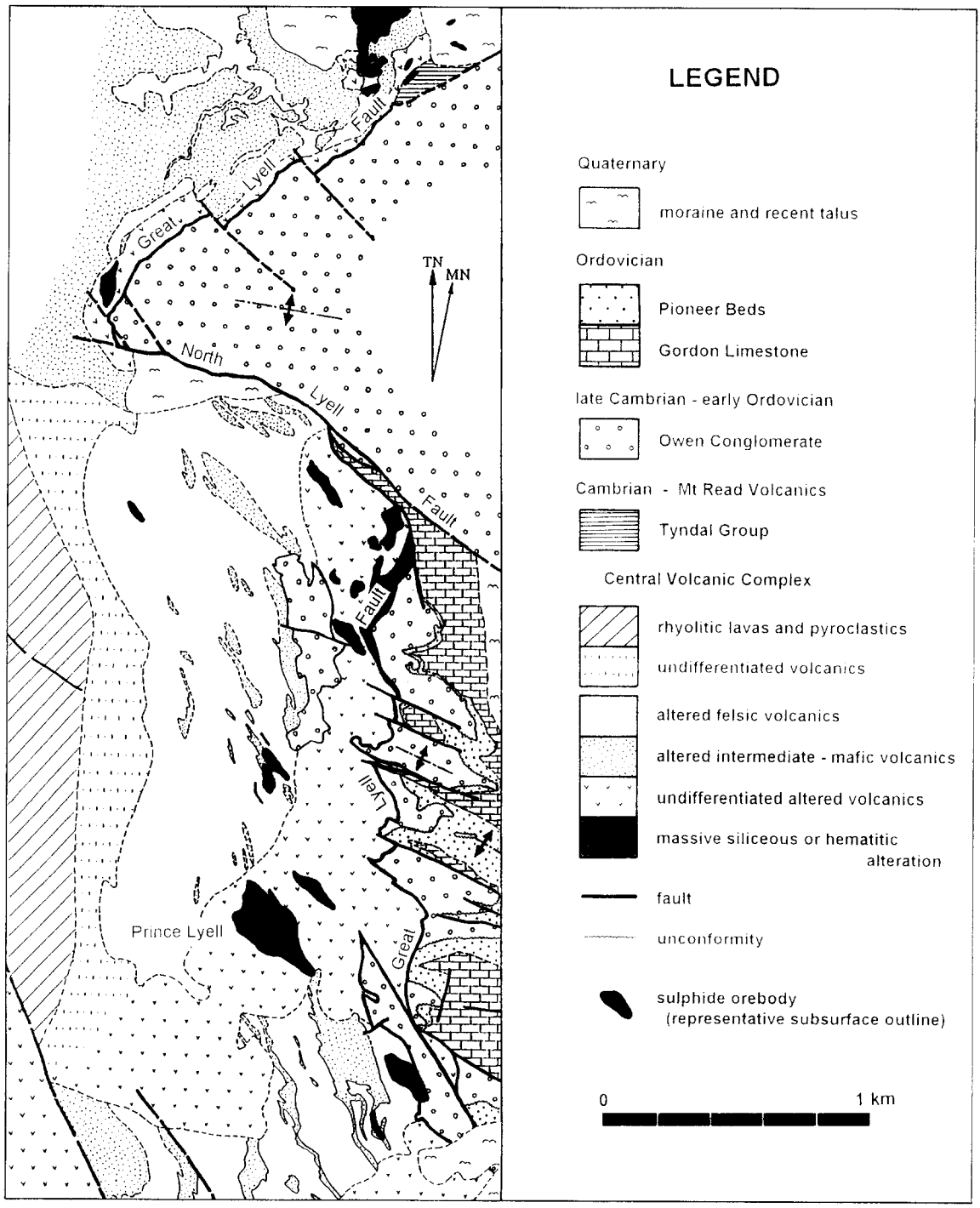

Fig. 2. Geology of the Mt Lyell mining field (compiled from Mt Lyell Mining and Railway Co. mapping).

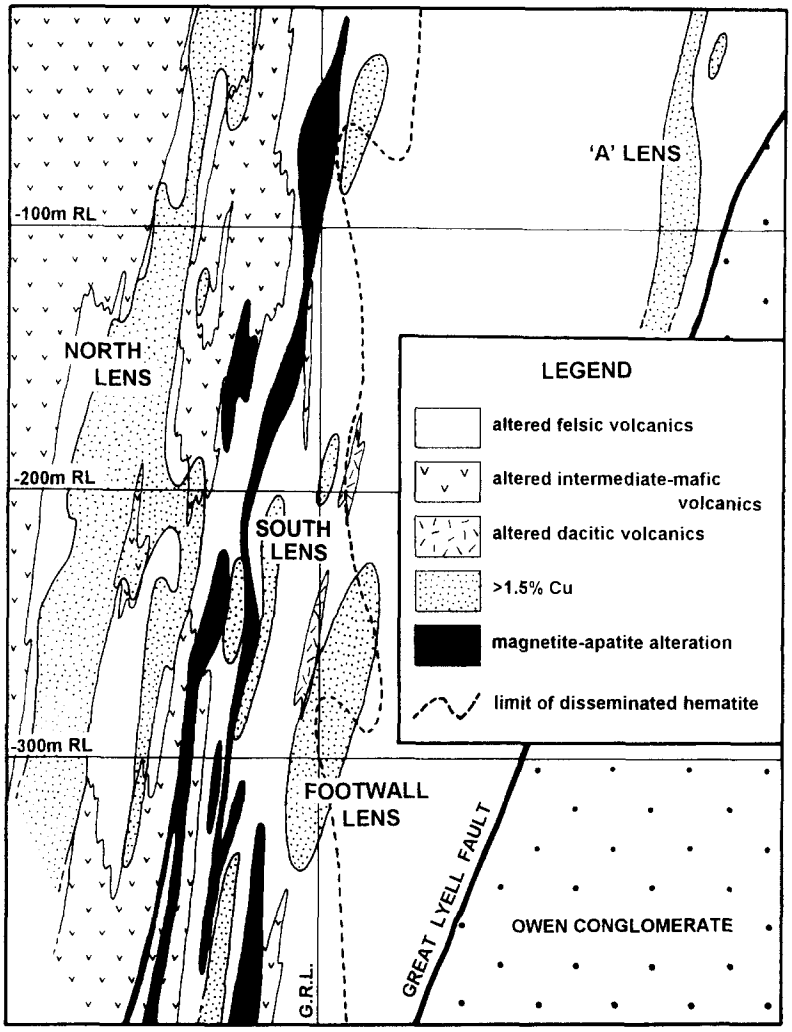

Fig. 3. Cross section (section 68, looking north–west) of the Prince Lyell and "A" Lens orebodies below zero RL. Copper mineralisation occurred mainly in the altered felsic volcanics between areas of altered intermediate-mafic volcanics.

ies of lead isotope ratios (Gulson and Porritt, 1987) confirmed a Cambrian connection, with ratios from Mt Lyell ores being similar to those from Cambrian VMS mineralisation at Rosebery, Hercules and Que River. The massive sulphide bodies at Mt Lyell were considered to be sea-floor exhalative mineralisation, while cogenetic disseminated sulphides formed by replacement of more permeable subsurface horizons (e.g., Reid, 1975; Walshe and Solomon, 1981). The mineralising fluids were thought to be circulating seawater that leached metals from the volcanic pile, and were localised by the junction of the proto-Great Lyell Fault and a Cambrian precursor to the Linda Disturbance. Sulphur was derived from reduced seawater sulphate with variable contributions from igneous rock sulphur (Solomon, 1976; Walshe and Solomon, 1981). Hematite–barite and silica–hematite alteration zones, associated with high grade bornite–chalcopyrite mineralisation adjacent to the Great Lyell Fault (Fig. 2), were thought by Solomon (1967) to be fossil gossans, developed from weathering of sulphides. Reappraisal of this alteration (Solomon, 1976; Walshe and Solomon, 1981) suggested that it may have formed from Cambrian fumarolic siliceous sinter deposits.

Considerable debate was rekindled in the mid

Devonian mineralisation (epigenetic or porphyry style)	Devonian mineralisation (Cambrian ore source?)	Cambrian mineralisation (volcanogenic)	Cambrian / Devonian (two phases of mineralisation)	Cambrian volcanogenic mineralisation with Devonian remobilisation
Gregory (1905)				
Hills (1927)				
Nye et al. (1934)				
Edwards (1939)				
Conolly (1947)				
Carey (1953)				
Bradley (1956)				
Wade and Solomon (1958)				
	Hall and Solomon (1962)			
	Solomon (1964)			
	Solomon and Elms (1965)			
		Solomon (1967, 1969, 1976)		
		Markham (1968)		
		McDonald (1968)		
		Green (1971)		
		Walshe (1971, 1977)		
		Jago et al. (1972)	Hendry (1972)	
		Reid (1975)		
		White (1975)		
		Bryant (1975)		
		Walshe and Solomon (1981)		
		Hendry (1981)		
		Cox (1981)		
		Corbett (1981, 1986)		
	Bird (1982)			
Brook (1984)				
Sillitoe (1984, 1985)				Arnold (1985)
		Gulson and Porritt (1987)		Solomon et al. (1987)
				Solomon and Carswell (1989)
				Hills (1990)
		Berry (1990b)		Arnold and Carswell (1990)

Fig. 4. Progression of Mt Lyell ore genesis theories since 1905.

1980's when a post-Cambrian, possibly metamorphic origin for the mineralisation was revived by consultant and mine geologists (Bird, 1982; Brook, 1984; Sillitoe, 1984, Sillitoe, 1985). These authors showed that alteration extended at least into the Owen Conglomerate and perhaps into the overlying Pioneer Beds. This led to theories of Devonian (or perhaps Ordovician) metamorphic or porphyry copper type ore formation by fluids focussed along the Great Lyell fault. Berry (1990b), however, considered the alteration to be absent above the Haulage Unconformity, constraining the age of the Mount Lyell mineralisation to pre-Pioneer Beds, invoking possible volcanogenic mineralisation during deposition of the Owen Conglomerate.

In order to explain the juxtaposition of pyrite–chalcopyrite and bornite–chalcopyrite ores, authors have invoked substantial in situ modification (e.g., Arnold, 1985; Arnold and Carswell, 1990) or remobilisation (e.g., Solomon et al., 1987) of Cambrian volcanogenic mineralisation by pre-D_2 Devonian metamorphic fluids circulating below the Haulage Unconformity. However, Devonian metamorphic fluids were unlikely to have added ore components to the Cambrian mineralisation (Solomon et al., 1987).

4. Alteration and mineralisation at Prince Lyell

The Prince Lyell deposit is hosted by steeply plunging, overturned, altered rhyolitic to dacitic volcanics at the contact with a sequence of altered

intermediate to mafic volcanics which form the stratigraphic footwall to the deposit. In general, alteration of the felsic lavas and breccias is texturally destructive, with embayed quartz phenocrysts being the only relict volcanic material. Sheared feldspar pseudomorphs may be preserved in less strongly altered dacitic lavas and relict fragmental textures are preserved in some coarse breccias. A "pseudofragmental" texture is imparted on these rocks by the development of siliceous alteration domains separated by a network of domains consisting of sericite + chlorite ± sulphides. The small-scale intercalation (a few centimetres to metres) of felsic and intermediate-mafic volcanics at their contact and relict breccia textures in the altered felsic units suggest that volcano-sedimentary units comprised a significant part of the volcanic pile.

The orebody is composed of a series of lenses: the North Lens, South Lens and Footwall Lens. The Footwall Lens is named according to the local mine terminology which refers to the present structural attitude of the mine sequence (i.e., overturned) and not its stratigraphic position. The distribution of sulphides is strongly controlled by the host lithologies. Intercalated intermediate-mafic and dacitic volcanics contain significantly less sulphides than the altered felsic units. Veinlet pyrite mineralisation in the intermediate-mafic volcanics increases irregularly towards their stratigraphic top from less than 5% up to 20% in some areas adjacent to the ore horizon. The rapid decrease in sulphide content stratigraphically below the orebody suggests there is no footwall feeder zone below the orebody. Instead, ore fluids appear to have moved laterally through more permeable units in the felsic volcanic pile.

In the ore lenses, disseminated and veinlet pyrite and chalcopyrite occur within quartz–chlorite–sericite altered rocks. Disseminated sulphides are concentrated within domains consisting of anastomosing networks of phyllosilicate alteration that separate relatively sulphide-free siliceous alteration domains. Pyrite is the dominant sulphide mineral and occurs as fractured anhedral to euhedral grains up to several millimetres across (Fig. 5A). Some areas of the orebody contain up to 30% pyrite, but concentrations of less than 10% are typical. Although the pyrite veinlets are mostly oriented sub-parallel to the stratigraphic layering and S_2, the strong layer-parallel

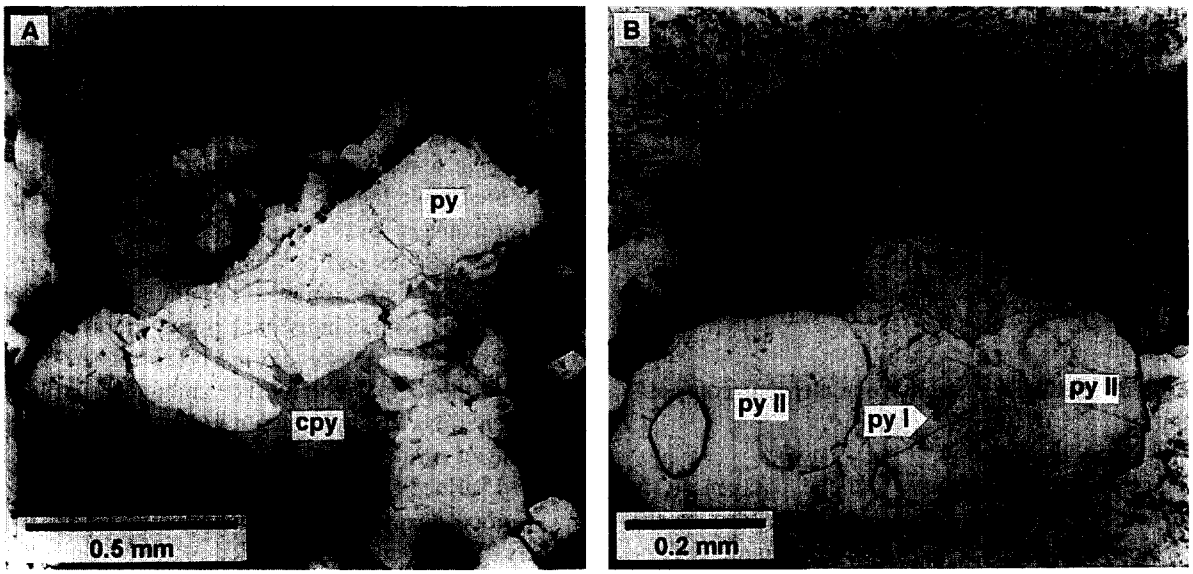

Fig. 5. (A) Fractured pyrite grains (py) with remobilised chalcopyrite (cpy) filling fractures and pressure shadows of pyrite (polished section 518307.9, PPL, unetched). (B) Pyrite grains showing different responses to etching due to crystallographic orientation. The upper grain is strongly pitted and displays no internal structure. The lower grain exhibits a core of corroded cobaltiferous Pyrite I overgrown by cobalt-poor Pyrite II containing abundant gangue mineral inclusions (polished section 115003, PPL, etched).

Devonian shearing is likely to have resulted in significant rotation of original veinlet orientations towards S_2.

Chalcopyrite most commonly occupies fractures and pressure shadows in and around pyrite grains (Fig. 5A). It also occurs without pyrite as intergrowths with the foliated phyllosilicate groundmass and may be smeared out along cleavage planes. No primary mineralisation textures can be interpreted from chalcopyrite as all textures are due to remobilisation during D_2 deformation. Rare grains of electrum are associated with chalcopyrite in fractured pyrite. Accessory minerals include disseminated magnetite, siderite, hematite, flourapatite and monazite.

Finely laminated textures are observed in discontinuous tabular bodies of massive pyrite ± chalcopyrite ± sphalerite ± galena and magnetite + quartz ± pyrite ± hematite. These textures are most likely the result of intense cleavage development within massive sulphides (Berry, 1990a) and incremental vein opening, although McDonald (1968), Arnold (1985) and Solomon and Carswell (in Corbett and Solomon, 1989) suggested that some sulphide bodies were the result of syngenetic sea-floor deposition. Highly elongate lenses of vein magnetite–apatite alteration replace chalcopyrite resulting in low grade regions in the orebody (Fig. 3) and may indicate the passage of a magmatic fluid (Raymond, 1992). Disseminated hematite ± siderite alteration in the structural footwall volcanics increases in intensity towards the Great Lyell fault (Fig. 3). A pervasive, extremely siliceous quartz–pyrite–minor sericite assemblage overprints the above alteration assemblages in the North Lens and in narrow zones in the South Lens.

5. Pyrite paragenesis and trace element composition

Interpretation of primary mineral paragenesis in the Mt Lyell field is often impossible due to the deformation or destruction of original mineral relationships during the major Devonian metamorphic event. Pyrite, on the other hand, is one of the few minerals that has not been entirely remobilised. Although much of the pyrite has been deformed by brittle fracture, minimal movement of pyrite fragments has occurred and internal structures are preserved.

Loftus-Hills and Solomon (1967) and Loftus-Hills (1968) were the first to investigate the geochemical characteristics of Prince Lyell pyrite in a regional study of the cobalt, nickel and selenium contents of western Tasmanian sulphides. Their work revealed contrasting trace element signatures of sulphides, especially pyrite, in a range of ore deposits and suggested that Cambrian volcanogenic and Devonian metamorphic deposits could be fingerprinted by their pyrite composition. Walshe (1971, Walshe (1977) and White (1975) also analysed trace elements in pyrite from the Mt Lyell field and the Mt Read Volcanics. Walshe (1977) noted some zoned pyrite at Prince Lyell and suggested that cobalt was not homogeneously distributed in pyrite.

The above mentioned works were carried out using wet chemical analyses of pyrite flotation separates, so that analyses were not selective of trace element variation within pyrite grains. As a result, many samples included multiple generations of geochemically distinct pyrite (see below). The present study has sought to combine the results of previous work with a detailed investigation of pyrite paragenesis and the composition of individual growth stages.

5.1. Internal structure of Prince Lyell pyrite

Polished sections of pyritic ore were etched for 30 to 60 s in a solution of sulphuric acid and $KMnO_4$ (modified after Ineson, 1989) to highlight the internal structure of pyrite grains. Etching of pyrite revealed a complex and previously unrecognised paragenesis of growth zoning, dissolution and multiple overgrowths within individual pyrite grains. Different pyrite generations could not be correlated on the basis of the depth of etching or amount of pitting in a given time, as the rate of etching of pyrite is dependant on the crystallographic orientation of the etched surface (Ramdohr, 1969) (Fig. 5B).

Composite pyrite grains commonly consist of a finely zoned core with corroded margins. Up to five subsequent generations of unzoned, anhedral to euhedral pyrite overgrowths may occur around the core, commonly separated by dissolution boundaries. Disseminated pyrite grains with no apparent internal

zoning or other structures are also common. Rarely, incremental widening of pyrite veinlets can be discerned with symmetrical growth of pyrite generations along the edges of the veins. By far the majority of the pyrite mineralisation is pre-S_2, with grains being fractured but not recrystallised by Devonian deformation. However, healing of brecciated pyrite grains by later pyrite and growth of pyrite in pressure shadows has also occurred on a very small scale.

5.2. Analytical methods

Over 400 trace element analyses of pyrite for Co, Ni, Cu, As, Ag, Zn and Se were performed on a Cameca SX-50 electron microprobe at the University of Tasmania. Optimum detection limits on the microprobe were 100 ppm for Co, Ni and Cu, 150 ppm for Ag, and 350 ppm for Zn and Se. Although individual generations and growth zones of pyrite could be analysed in this way, detection limits were far higher than for earlier bulk pyrite studies mentioned above which employed wet chemical methods. Overlap of the Pb L_α peak on the As K_α peak resulted in a skewed As distribution with few analyses below 300 ppm. This suggests that the Pb overlap inflated the As data by around 300 ppm and consequently As data were regarded as semi-quantitative only.

5.3. Copper, zinc, silver, selenium and arsenic in pyrite

Most of the analyses for Zn, Ag and Se and a high proportion of the Cu data were below the detection limits for this study. The distributions of Zn and Cu above the detection limits were erratic and in most cases were interpreted to be due to submicroscopic inclusions of sphalerite and chalcopyrite in the pyrite. However, high Zn levels were recorded in pyrite from a sphalerite–barite vein where it is probable that Zn diffused into the pyrite lattice from the enclosing sphalerite. Pyrite with levels of Cu consistently above detection limits was observed in only one sample; the host rock did not contain significant chalcopyrite and it is not clear why the pyrite in this sample should have contained uniformly high levels of Cu.

The lack of Ag and Se data above detection limits prevented a meaningful interpretation of their distribution. No samples contained pyrite with consistent levels above detection limits and no further consideration of these data was given. Pyrite containing high levels of arsenic was observed within a zone of silicification from the northern part of the South Lens. The pyrite contained up to around 1% As, with levels of all other trace elements below detection limits. The consistently high arsenic analyses within grains suggested that arsenic was contained in solid solution in the pyrite lattice and not as inclusions of arsenopyrite.

5.4. Cobalt and nickel in pyrite

In general, cobalt and nickel are the most common trace elements found in pyrite, exhibiting extensive isomorphous solid solution with iron (Fleischer, 1955; Hawley and Nichol, 1961; Riley, 1968). Both cobalt, and to a lesser extent nickel, are strongly chalcophile and are preferentially incorporated into the pyrite structure relative to iron (Springer et al., 1964). Complete substitution of cobalt for iron (pyrite–cattierite series) is not achieved at temperatures below 700°C. However, up to 9 wt% Co can be accommodated in the pyrite structure up to 400°C under equilibrium conditions (Klemm, 1962). Almost all ratios of Co:Ni:Fe occur in nature (Springer et al., 1964). Brown and Bartholmé (1972) observed up to 20 wt% Co in Zambian copper belt pyrite, but suggested that such high cobalt levels were metastable and the result of disequilibrium conditions during deposition.

The Co:Ni ratio in pyrite has been used by many authors as an empirical indicator of the environment of pyrite deposition. Although regarded by some as of dubious value to ore genesis interpretation (e.g., Campbell and Ethier, 1984), Co:Ni ratios of less than one with a low standard deviation are generally accepted to represent pyrite of sedimentary origin. Low cobalt and nickel concentrations are also characteristic of such pyrite. Conversely, highly variable Co:Ni ratios, usually greater than one, are thought to be the result of hydrothermal mineralisation (Bralia et al., 1979).

At Prince Lyell, cobalt and nickel are by far the most abundant and useful trace elements for discerning chemically distinct generations of pyrite. These

elements exhibit relatively uniform distribution within growth zones and individual pyrite overgrowths, indicating their inclusion in the pyrite structure in solid solution rather than as mineral inclusions. However, levels of cobalt and nickel do not show sympathetic variation (Fig. 6), indicating that equilibrium partitioning did not occur, probably due to undersaturation of one or both of the elements with respect to pyrite. This undersaturation meant that buffering of the cobalt and/or nickel concentration in the ore fluid could not occur, with rapid variation of cobalt and nickel concentrations as new pulses of hydrothermal fluid were introduced or physicochemical conditions varied. Equilibrium concentrations of cobalt in pyrite under saturation conditions would also be significantly higher than those observed at Prince Lyell (Klemm, 1962).

Despite the poor correlation between the elements in solid solution, the concentrations of cobalt, and to a lesser extent nickel, exhibit the most consistent relations of all the trace elements to different pyrite morphologies. Three main groups of pyrite have been defined on the basis of cobalt content and morphology and are described below.

5.4.1. Pyrite I

Pyrite I, forming the cores of many composite pyrite grains, exhibits idiomorphic oscillatory growth zoning (Figs. 7 and 8). Individual growth zones may be as narrow as 0.5 μm. The margins of Pyrite I are characteristically corroded and euhedral outlines are very rarely preserved. Grains which show only a small degree of dissolution have complex finely zoned cores followed by simpler wider growth zones nearer the margins.

Growth zones contain cobalt at levels generally between 1000 and 10,000 ppm, although some zones may have as low as 300–500 ppm cobalt. In the few specimens where the outer, wider zones have not been corroded, there is a poorly defined trend towards lower cobalt values in the outer zones. Nickel concentrations in Pyrite I are variable, ranging from below detection limits (< 100 ppm) to almost 5000 ppm. The majority of Pyrite I contains very little arsenic. Some elevated arsenic levels were observed in inner zones of Pyrite I which were also very high in cobalt, however, no overall correlation of arsenic and cobalt was observed.

No diffuse zoning of trace elements was observed in pyrite (Figs. 7 and 8), although the behaviour of trace elements at very low levels (< 100 ppm) could not be examined. Compositional changes across dissolution boundaries were sharply defined. This indicates that in situ redistribution of trace elements in pyrite did not occur during the lower greenschist Devonian metamorphism. This is consistent with the findings of other authors (e.g., Brown and Bartholmé, 1972; Itoh, 1973; Fleet et al., 1988) who found that primary compositional heterogeneities in pyrite appear to be preserved through low grade metamorphism.

A few grains of Pyrite I contain small inclusions of pyrite with very high cobalt levels, up to 3% Co.

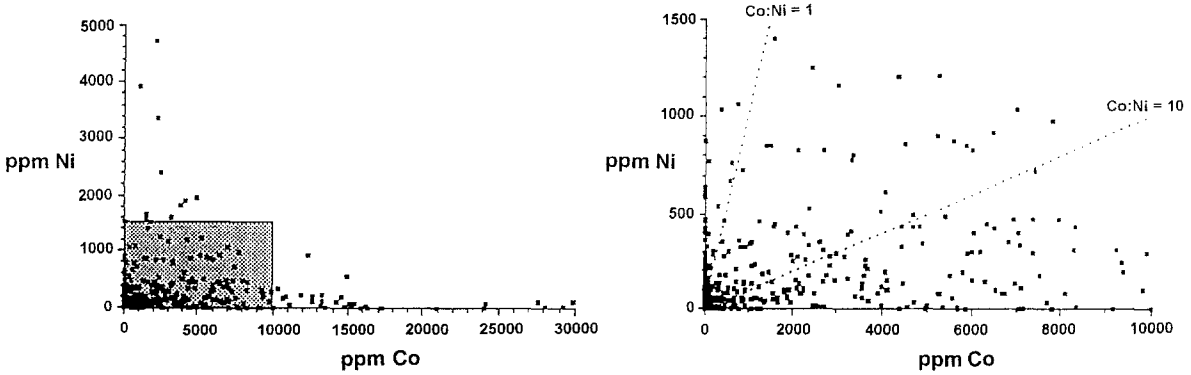

Fig. 6. (left) Plot of cobalt and nickel concentrations from 413 electron microprobe analyses of Prince Lyell pyrite, illustrating the lack of correlation between the two trace elements. (right) Detail of shaded. Co:Ni ratios are highly variable with the majority being greater than one.

These inclusions may be the remnants of a very early cobaltiferous pyrite, evidence of which has been almost entirely removed by dissolution by later fluids. Pyrite I rarely contains gangue mineral inclusions, which are commonly clustered around the margins of Pyrite I cores within later pyrite overgrowths.

Hematite inclusions do not occur in Pyrite I. However, in areas of disseminated hematite alteration of the host rock, hematite inclusions occur

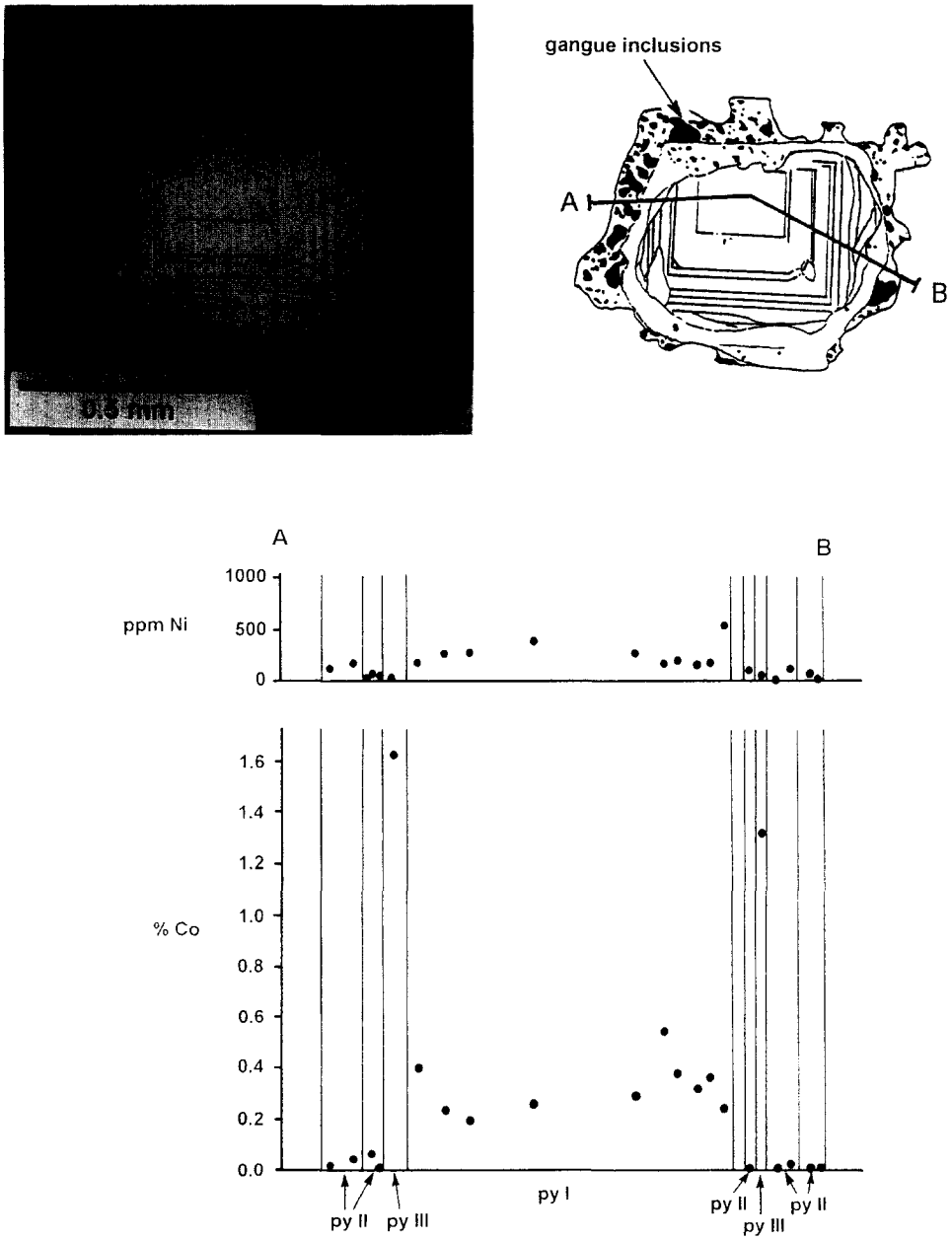

Fig. 7. Electron microprobe traverse across a complex pyrite grain showing cobalt and nickel distribution. Multiple generations of cobalt-poor Pyrite II and cobalt-rich Pyrite III overgrow a zoned and corroded core of Pyrite I (polished section 618051.0, PPL, etched).

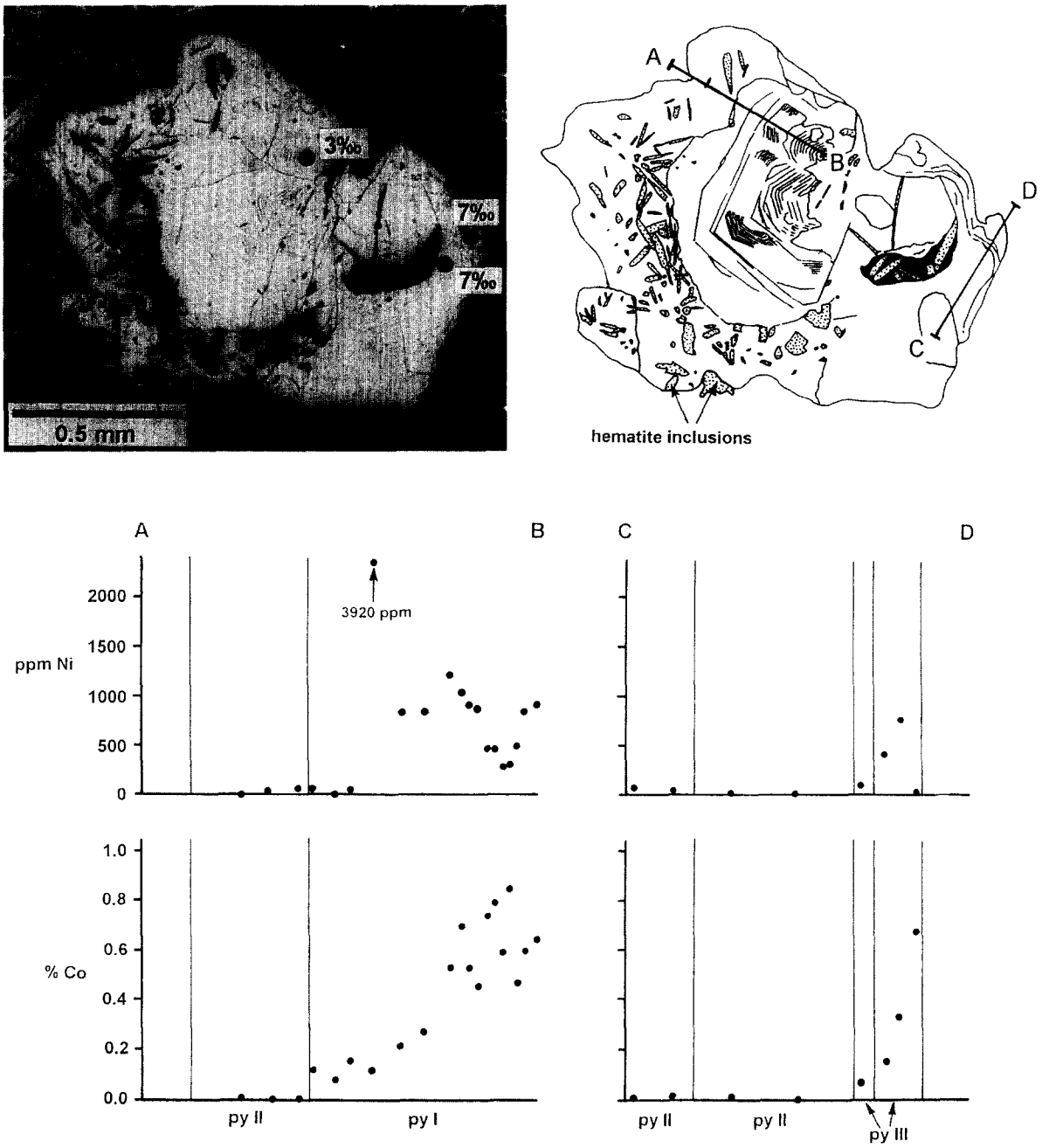

Fig. 8. Electron microprobe traverses across a complex pyrite grain showing cobalt and nickel distribution. Pyrite I becomes less cobaltiferous in wider zones towards its margin. Pyrite II contains abundant bladed hematite inclusions and is overgrown by thin Pyrite III rims in part. SHRIMP $\delta^{34}S$ ratios in all three pyrite types are also shown (polished section 599377.3, PPL, etched).

around Pyrite I grain margins enclosed by later pyrite overgrowths (Fig. 8). This relationship indicates that Pyrite I was earlier than hematite and is in contrast to the suggestion of Walshe and Solomon (1981) that the bulk of hematite alteration was an early pre-sulphide event.

5.4.2. Pyrite II

The term "Pyrite II" does not refer to a single episode of pyrite deposition. Several overgrowths of Pyrite II can occur within a single composite pyrite grain (Figs. 6 and 7) and there may be dissolution boundaries between them. Pyrite II does not have internal zoning and typically contains cobalt and nickel at levels below the detection limits for this study (< 100 ppm). It is volumetrically by far the most common type of pyrite in the southern part of the Prince Lyell deposit.

Pyrite II forms euhedral to anhedral overgrowths on Pyrite I cores, but may also form discrete disseminated pyrite euhedra and irregular grains. No evidence was observed of any Pyrite II predating Pyrite I. Fractured grains of Pyrite II occur where Pyrite II veinlets have been dismembered by shearing along the Devonian cleavage. Where dissolution boundaries between generations of Pyrite II are not highlighted by etching, lines of gangue inclusions may define overgrowth boundaries (Figs. 7 and 8). Pyrite II contains many types of inclusions, including quartz, sericite, chlorite, siderite, apatite, magnetite, hematite, monazite and rutile. Inclusions of sphalerite and galena were also observed in samples of Pyrite II from the Great Lyell fault zone.

5.4.3. Pyrite III

Pyrite III is a small but important pyrite population at Prince Lyell. It occurs as thin unzoned, anhedral overgrowths on Pyrite I and II, and as minor veinlets. It typically contains cobalt above 5000 ppm, but rarely as low as 500 ppm (Figs. 7 and 8). As with all the cobaltiferous pyrite at Prince Lyell, nickel contents are variable, ranging from < 100 to 800 ppm. Repeated thin rims of Pyrite II and Pyrite III may overgrow each other within a single pyrite grain, reflecting variations in the composition of the mineralising fluids.

6. Sulphur isotope ratios of Prince Lyell pyrite

Study of down-dip and across-dip $\delta^{34}S$ variation was carried out. Conventional analyses of pyrite separates were carried out by the method of Robinson and Kusakabe (1975), with precision of $\pm 0.75‰$ or better. These samples were obtained by drilling

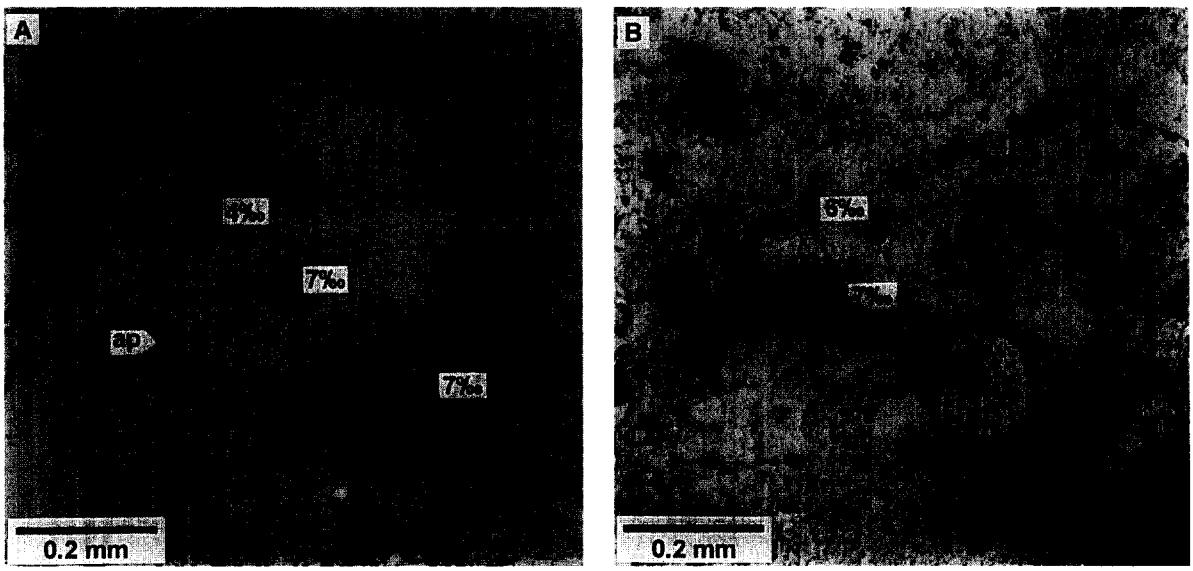

Fig. 9. Internal textures and SHRIMP $\delta^{34}S$ ratios of Prince Lyell pyrite. (A) Corroded Pyrite I core (7‰), overgrown by two more euhedral Pyrite I generations (7‰) and anhedral finally anhedral Pyrite II (4‰). Apatite (ap) inclusion occurs in Pyrite II at the margin of Pyrite I. Chalcopyrite (dark coloured due to the etching process) occurs in the pyrite pressure shadow (polished section 115003, PPL, etched). (B) Finely zoned and corroded Pyrite I (6‰) overgrown by anhedral, cobalt-rich Pyrite III (7‰) (polished section 589259.7, PPL, etched).

Table 1
Conventional sulphur isotope analyses of Prince Lyell pyrite

Sample no.	$\delta^{34}S$ (‰)	Sample no.	$\delta^{34}S$ (‰)
115002A	5.9	619055.3	7.2
115002B	8.8	619086.8	6.8
568A289.5	8.5	619134.0	8.3
584326.5	7.3	622095.5	7.4
584389.0	7.8	624050.4	10.8
596320.7	7.4	634044.4	7.9
596343.9	7.9	634085.6	7.3
596401.6	9.0	634131.0	7.0
596431.6	9.1	635010.0	7.3
596454.8	9.8	635024.4	6.3
605023.0	8.9	635069.9	7.3
605050.2	7.3	635085.0	10.8
605074.1	7.9	635130.4	8.1
607068.8	11.1	636040.9	8.5
607104.3	7.6	637029.6	9.2
619017.3	8.1	698100.4	7.6

Other $\delta^{34}S$ data used in this study: (i) Solomon et al. (1969): 8 samples, range +6.3–10.0‰, mean +8.0‰. (ii) Walshe and Solomon (1981): 13 samples, range +5.6–8.7‰, mean +7.2‰.

pyrite from polished blocks after microscopic inspection to eliminate impurities and were not selective of any individual pyrite generations. These analyses were used in conjunction with previous bulk pyrite $\delta^{34}S$ studies from shallower levels at Prince Lyell (Solomon et al., 1969, Solomon et al., 1988; Walshe, 1977; Walshe and Solomon, 1981) to determine spatial variation of $\delta^{34}S$ ratios in and around the orebody.

Secondly, in situ $\delta^{34}S$ microanalysis was carried out using the SHRIMP ion microprobe at the Australian National University, Canberra. The $\delta^{34}S$ values of sulphur ions, liberated from a site 30–40 μm wide and 10 μm deep on a polished pyrite sample, were analysed with an analytical error of ± 2‰ (Eldridge et al., 1989). The technique enabled investigation of $\delta^{34}S$ variation between different generations of pyrite growth (Figs. 8 and 9), albeit with less precision than conventional methods.

The distribution of conventional pyrite $\delta^{34}S$ ratios is tightly constrained around a maximum at 7–8‰, with a range from 5.6 to 11.1‰ (Table 1). This range is consistent with a mixed Cambrian seawater ($\geq$ 10‰) and igneous rock ($\sim$ 0‰) reduced sulphur source. The data show no zonation either down dip or along the strike of the orebody, apart from a poorly defined central core of lighter values ($\delta^{34}S < 8$‰) corresponding to the copper mineralised zone. Values above 8‰ generally occur in the hangingwall and footwall rocks to the ore horizon. The zonation to lighter values may reflect a greater contribution to the copper mineralising fluid from igneous sulphur, relative to the fluid depositing the more widespread pyrite alteration. Large et al. (this volume) document other evidence for a possible magmatic influence in Prince Lyell copper mineralisation. Alternatively, the zonation may reflect a gradual change in $\delta^{34}S_{\Sigma S}$ of the hydrothermal fluid as lighter igneous rock sulphur contributed less to a seawater-derived fluid over time (see Green et al., 1981; Solomon et al., 1988). By this process, later formed isotopically heavier pyrite may have been deposited as the fluid permeated further into the wallrocks.

A greater variation in $\delta^{34}S$ values may have been expected from the SHRIMP analyses, given that the mixed provenance of conventional $\delta^{34}S$ analyses would have resulted in averaging of $\delta^{34}S$ values of discrete pyrite generations. The range of values was from 3‰ to 9‰ (Table 2), with four analyses falling outside the range of the conventional method. However, taking into account analytical error (± 2‰), these values fall close to or within the range of bulk pyrite analyses. There is no evidence to suggest that sulphur was derived from a source other than reduced Cambrian seawater sulphate ($\geq$ 10‰) with

Table 2
SHRIMP $\delta^{34}S$ analyses of Prince Lyell pyrite

Sample no.	Pyrite type	$\delta^{34}S$ (‰)
115003	I	7
115003	I	7
115003	II	4
598259.7	I	6
598259.7	III	7
599377.3	I	3
599377.3	II	7
599377.3	III	7
619098.6	II	9
619098.6	III	8
619098.6	II	9
624096.9	I	6
624096.9	II	6
639121.3	I	4
639121.3	II	5

some influence from Cambrian igneous rock sulphur ($\sim 0‰$).

No consistent $\delta^{34}S$ variation was observed between individual pyrite generations. For example, sample 115003 showed a decrease in $\delta^{34}S$ from cobalt-rich core to cobalt-poor rim, whereas sample 599377.3 showed the reverse trend (Figs. 8 and 9). The highest SHRIMP $\delta^{34}S$ values occurred in sample 619098.6 from a zone of late overprinting quartz–pyrite alteration and may reflect a lower temperature of the hydrothermal fluid at this time.

7. Implications of pyrite composition for pyrite–chalcopyrite mineralisation

7.1. The pyrite–chalcopyrite association

The association of cobaltiferous pyrite and high, variable cobalt/nickel ratios with volcanic rocks and volcanogenic sulphide deposits has been established in western Tasmania (Loftus-Hills, 1968; White, 1975) and elsewhere (e.g., Bralia et al., 1979), suggesting a volcanogenic origin for Pyrite I and III. A positive correlation of cobaltiferous pyrite with copper mineralisation was established at Prince Lyell by Walshe (1977) (fig. 26 in Walshe and Solomon (1981)). This is consistent with numerous studies in Tasmania and elsewhere which have documented the association of cobaltiferous pyrite with copper mineralisation (e.g., Loftus-Hills, 1968; Bartholmé et al., 1971; Itoh, 1973). Green et al. (1981) also noted a zone of highly cobaltiferous pyrite in the altered footwall volcanics of the Rosebery massive sulphide deposit and interpreted it as a conduit for volcanogenic hydrothermal fluids. Although there is no textural evidence to link a single pyrite generation to chalcopyrite at Prince Lyell due to the metamorphic remobilisation of chalcopyrite, the relationship between the cobalt content of pyrite and copper grade suggests chalcopyrite was deposited with cobaltiferous pyrite.

The oscillatory zoning of Pyrite I may reflect fluctuations in temperature, pH or fO_2 of the hydrothermal fluid during volcanogenic mineralisation (Klemm, 1962; Walshe, 1977). Bogush (1983) regarded compositional zoning such as that displayed by Pyrite I to be uncharacteristic of pyrite of metamorphic origin. Fluctuations in fluid parameters are not expected from a regional metamorphic fluid which evolved in equilibrium with the host rocks.

The timing of Pyrite II (after Pyrite I) inferred here differs from that proposed by Walshe (1977) who suggested that deposition of cobalt-poor pyrite was followed by cobalt-rich pyrite in response to a drop in fO_2 and increase in pH accompanying chalcopyrite mineralisation. It is possible that the contrasting low cobalt composition of Pyrite II was due to a significant drop in temperature or pH resulting in a lesser amount of cobalt partitioning into pyrite. However, it is more likely that the principal factor was a lower primary concentration of cobalt in the fluid (Fleischer, 1955; Loftus-Hills, 1968; Barton, 1970). This may reflect a decrease in temperature or salinity, both of which could suppress the solubility of cobalt and copper in the hydrothermal fluid. Alternatively, or as well, it may have been caused by an influx of volcanogenic fluid which had derived little cobalt and copper from an already strongly leached volcanic pile. Minor sporadic pulses of a more mineralised fluid would have resulted in the deposition of cobaltiferous Pyrite III, possibly due to the fluid passing through different pathways in the volcanics.

7.2. The hematite–pyrite association

Disseminated hematite ± siderite alteration is common in the structural footwall rocks of Prince Lyell and becomes markedly stronger towards the contact with the hematite-bearing Owen Conglomerate. The Great Lyell fault zone is commonly strongly hematitic and has most probably acted as a focus for the hematite alteration fluid. Hematite alteration zones further from the Great Lyell fault at Prince Lyell and Western Tharsis were probably formed by the fluid moving away from the fault along permeable horizons in the volcanics. The presence of the Great Lyell fault during this alteration implies that the growth faulted margin of the Owen Conglomerate basin had formed during mineralisation at Prince Lyell.

The hematite may have been deposited by a fluid derived from the evolving volcanogenic hydrothermal system as it cooled and reductants in the volcanic pile were consumed, with the fluid focussed

along the Great Lyell fault. An alternative source of an oxidised fluid for hematite alteration at this time could have been basin fluids from dewatering of the Owen Conglomerate. Erosion of hematite-altered volcanics into the basin may account for hematitic detritus in the Owen Conglomerate reported by Solomon (1967).

Hematite blades occur as inclusions in Pyrite II and III, but not in Pyrite I. Although Walshe and Solomon (1981) documented some pyrite replacing hematite, the hematite inclusions in Pyrite II and III are in apparent equilibrium with the pyrite with no evidence of replacement textures. The presence of hematite inclusions in Pyrite II and III implies that this pyrite was deposited after formation of the Great Lyell growth fault, constraining the age of Pyrite II and III to late Cambrian–early Ordovician or younger.

Pyrite II mineralisation from a Devonian metamorphic fluid is a possibility (Fig. 10A). Its cobalt-poor composition is similar to that of pyrite and other sulphides typically associated with Devonian mineralisation and granitoids in western Tasmania (e.g., Loftus-Hills, 1968; Patterson et al., 1981). The similar $\delta^{34}S$ ratios in all Prince Lyell pyrite indicate that any Devonian mineralisation event would have recycled Cambrian volcanogenic sulphur and there is ample textural evidence for dissolution of early volcanogenic Pyrite I to provide that sulphur. Cobalt in early formed Pyrite I would have been expelled from the pyrite lattice during dissolution and redeposition as Pyrite II. Loftus-Hills (1968) demonstrated that pyrite remobilised from altered volcanics into Devonian metamorphic quartz veins contained far less cobalt than pyrite in the host volcanics. This trend of cobalt depletion in remobilised metamorphic pyrite is mirrored by the in situ diffusion of cobalt out of the pyrite lattice observed in moderate to high metamorphic grade rocks (Bartholmé et al., 1971; Brown and Bartholmé, 1972; Itoh, 1973).

A Devonian age for Pyrite III is more difficult to sustain. The repeated overgrowths of Pyrite II and Pyrite III in some pyrite grains would require the deposition of both cobalt-poor and cobalt-rich pyrite from the metamorphic fluid. Cobaltiferous Pyrite III may have resulted from local concentrations of cobalt liberated during Pyrite I dissolution. However, its cobalt-rich composition is in stark contrast to that of cobalt depletion observed in Devonian pyrite mineralisation in western Tasmania.

7.3. An Ordovician mineralisation scenario

The relationship between hematite and pyrite may be explained by considering that the last stages of Mt Read volcanism were active during deposition of the Owen Conglomerate in the late Cambrian to early Ordovician. However, the small amount of volcanic detritus in the conglomerate suggests that eruptive volcanic activity had ceased by the time Owen Conglomerate sedimentation commenced and suggests that volcanic activity was restricted only to subsurface circulation of fluids in the volcanic pile heated by subvolcanic plutons. The notion of Cambrian volcanism and hydrothermal activity continuing into the early Ordovician has been suggested by several authors (e.g., Sillitoe, 1985; Berry, 1990b). Jago et al. (1977) reported early Ordovician Mt Read-type intrusive rocks in the Dial Range area, some 100 km northwest of Mt Lyell. Sillitoe (1985) noted that if alteration observed in the Owen Conglomerate was of volcanogenic origin, it would require rapid accumulation of the conglomerate in the typical life time of a hydrothermal system ($\sim$ 2–3 million years). It is possible also, that fluid circulation was promoted by local deformation of the Mt Read Volcanics and Owen Conglomerate during formation of the Haulage unconformity in the early Ordovician.

In this hematite mineralisation scenario (Fig. 10B), an oxidised fluid from the waning volcanogenic hydrothermal system, or perhaps an Owen Conglomerate formation water, was focussed along the Great Lyell fault margin of the sedimentary basin, and migrated back into the volcanic hydrothermal system. A volcanogenic fluid could have been initially oxidised as a normal consequence of a cooling hydrothermal system or could have become oxidised as it interacted with the Owen Conglomerate as it was channelled along the faulted contact. Hematite would have been deposited as the fluid was back circulated along permeable horizons in the volcanics.

Alternatively, an oxidised connate fluid, derived from dewatering of the hematitic Owen Conglomerate, would have encountered an abrupt redox change across the Great Lyell fault and may have dissolved pyrite and deposited hematite in the volcanics. There

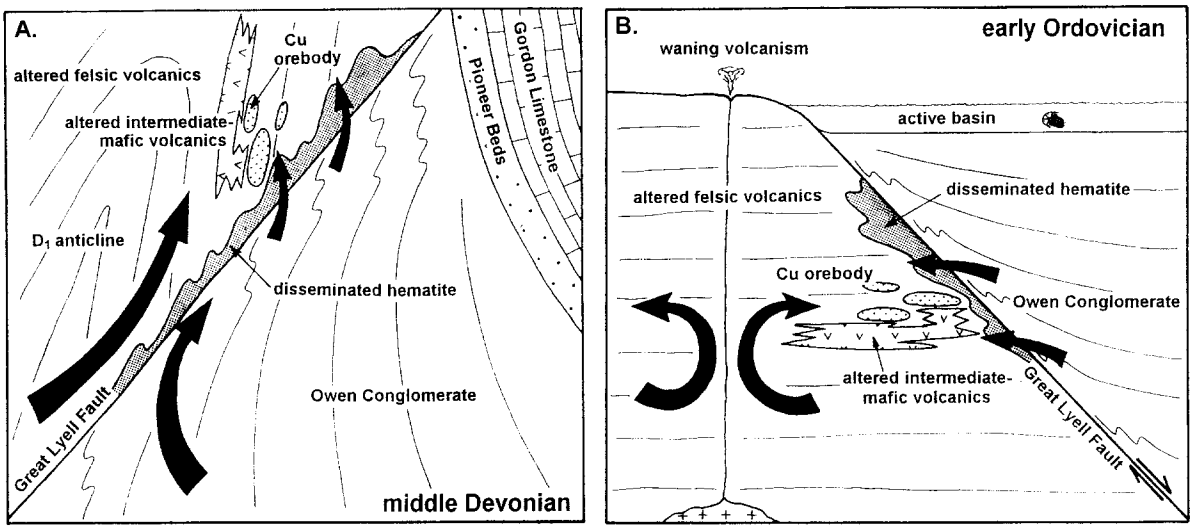

Fig. 10. (A) Scenario for Pyrite II and III and hematite mineralisation during Devonian metamorphism. An oxidised metamorphic fluid from the Owen Conglomerate deposited disseminated hematite in the footwall volcanics while Pyrite I was corroded and redeposited as Pyrite II and III. (B) Scenario for Pyrite II and III and hematite mineralisation during the early Ordovician. Volcanic activity was limited to circulation of subsurface fluids heated by subvolcanic plutons. Hematite was deposited from fluids either from the cooling hydrothermal system or from dewatering of the Owen Conglomerate which were focussed along the Great Lyell fault and into the volcanic pile.

is no evidence of very low or negative $\delta^{34}S$ values which may be expected of later pyrite (Pyrite II and III) deposited in equilibrium with hematite (Ohmoto and Rye, 1979). However, a fluid could have dissolved Pyrite I and precipitated it as Pyrite II with similar $\delta^{34}S$ ratios under essentially closed system conditions, deriving the bulk of its sulphur from dissolution of the pre-existing pyrite. Alternatively, with a minor influx of oxidised fluid relative to a dominant reduced volcanogenic fluid and with little mixing of the two, Pyrite II and III could have been deposited from the volcanogenic fluid in disequilibrium with the hematite-bearing fluid.

Significantly lower pyrite $\delta^{34}S$ ratios occur in the strongly hematitic North Lyell orebodies (Walshe and Solomon, 1981) and are more consistent with re-equilibration of a hydrothermal fluid with a more oxidised, open environment. This feature raises the possibility that much of the mineralisation along the Great Lyell fault in the North Lyell area may have been concentrated by an oxidation–reduction trap. Hot, reduced volcanogenic fluids circulating through the volcanic pile would have encountered a cooler, oxidised environment at the growth fault contact with the Owen Conglomerate. Mixing with oxidised basin waters which migrated along and across the Great Lyell fault could also have initiated precipitation of sulphides from the hydrothermal fluid.

8. Summary

The trace element and stable isotope geochemistry of Prince Lyell pyrite suggests that pyrite associated with chalcopyrite was precipitated from a volcanogenic hydrothermal fluid. The predominantly seawater-derived fluid was focussed along permeable horizons in the felsic volcanic pile and deposited veinlet and disseminated mineralisation. Early mineralisation produced cobaltiferous Pyrite I and chalcopyrite. The bulk of the pyrite (Pyrite II) was deposited after chalcopyrite mineralisation by fluids poor in base metals. As a result of fluctuations in physico-chemical conditions of the fluid, generations of early formed pyrite were repeatedly corroded and reprecipitated forming composite pyrite grains.

While eruptive volcanism may have ceased in the late Cambrian, it is postulated that hydrothermal fluids heated by a subvolcanic granite continued to circulate within the volcanic pile into the early Or-

dovician. An oxidised hydrothermal fluid or perhaps connate water from dewatering of the Owen Conglomerate basin was focussed along the growth-faulted basin margin and deposited disseminated hematite in the volcanics adjacent to the Great Lyell fault and along permeable horizons in the volcanic pile.

Deposition of pyrite continued in the altered volcanics from fluids poor in copper and cobalt, deriving sulphur primarily from the dissolution of earlier formed pyrite, preserving the $\delta^{34}S$ ratios of the precursor pyrite. Episodic recharging of the fluid with metals such as cobalt and copper resulted in the deposition of small amounts of cobalt-rich Pyrite III and chalcopyrite.

The interaction of reduced volcanogenic fluids with the redox boundary formed by the Great Lyell fault and mixing with oxidised Owen Conglomerate basin waters provide possible mechanisms for mineralisation along the length of the Great Lyell fault.

Acknowledgements

This paper presents the results of research conducted for a Master of Science at the Centre for Ore Deposit and Exploration Studies (CODES), University of Tasmania supported by an Australian Postgraduate Award and a Tasmanian Mining Industry Scholarship. The supervision and advice of Prof. R.R. Large and CODES staff are gratefully acknowledged. Drs. J.L. Walshe and M. Solomon also provided valued constructive comments. I wish to thank the Mt Lyell Mining and Railway Company for their generous support during this study. I also extend my thanks to Dr. S. Eldridge for analyses carried out on the SHRIMP ion microprobe at the Australian National University and to W. Jablonski for his instruction on the electron microprobe. This paper is published with the permission of the Director, Australian Geological Survey Organisation.

References

Arnold, G.O., 1985. Mt. Lyell 1985: an exploration perspective. Unpublished report, Gold Fields Exploration Pty Ltd, Queenstown, Tasmania.

Arnold, G.O. and Carswell, J.T., 1990. The Mt Lyell deposits. In: K.R. Glasson and J.H. Rattigan (Editors), Geological Aspects of the Discovery of Some Important Mineral Deposits in Australia. Australas. Inst. Min. Metall. Monogr., 17: 135–140.

Bartholmé, P., Katekesha, F. and Lopez-Ruiz, J., 1971. Cobalt zoning in microscopic pyrite from Kamoto, Republic of the Congo (Kinshasa). Miner. Deposita, 6: 167–176.

Barton, P.B. jnr, 1970. Sulphide petrology. Mineral. Soc. Am., Spec. Pap., 3: 187–198.

Berry, R.F., 1990a. Structure of the Rosebery deposit. Structure and Mineralisation of Western Tasmania. Unpublished AMIRA project report, P291, pp. 17–26.

Berry, R.F., 1990b. Structure of the Queenstown area and its relation to mineralisation — interim report. Structure and Mineralisation of Western Tasmania. Unpublished AMIRA project report, P291, pp. 27–68.

Berry, R.F. and Crawford, A.J., 1988. The tectonic significance of Cambrian allocthonous mafic–ultramafic complexes in Tasmania. Aust. J. Earth Sci., 35: 523–533.

Bird, M., 1982. An assessment of the economic geology of Mt Lyell. Unpublished report, Mt Lyell Mining and Railway Co. Ltd, Queenstown, Tasmania.

Bogush, I.A., 1983. Evaluation of productivity and mode of functioning of endogene sulphide-ore sources on the basis of growth zoning in pyrite. Doklady, Acad. Sci. USSR, 258: 149–154.

Bradley, J., 1956. The geology of the West Coast Range of Tasmania, Part II — Structure and ore deposits. Papers Proc. R. Soc. Tasmania, 90: 65–130.

Bralia, A., Sabatini, G. and Troja, F., 1979. A revaluation of the Co/Ni ratio in pyrite as a geochemical tool in ore genesis problems. Miner. Deposita, 14: 353–374.

Brook, W.A., 1984. Mineralisation at Mt Lyell and exploration of the buffer zone, mine lease and E.L. 9/66. Unpublished report, Gold Fields Exploration Pty Ltd, Queenstown, Tasmania.

Brown, A.C. and Bartholmé, P., 1972. Inhomogeneities in cobaltiferous pyrite from the Chibuluma Cu–Co deposit, Zambia. Miner. Deposita, 7: 100–105.

Bryant, C.J., 1975. The geology and mineralisation of the corridor area, Mt Lyell, Tasmania. Unpublished B.Sc. (Hons.) Thesis, University of Tasmania.

Campbell, F.A. and Ethier, V.G., 1984. Nickel and cobalt in pyrrhotite and pyrite from the Faro and Sullivan orebodies. Can. Mineral., 22: 503–506.

Carey, S.W., 1953. Geological structure of Tasmania in relation to mineralisation. In: A.B. Edwards (Editor), Geology of Australian Ore Deposits, 5th Empire Mining and Metallurgical Congress Publication, Vol. 1, pp. 1108–1128.

Connolly, H.J.C., 1947. Geology in exploration: Mount Lyell example. Pr oc. Australas. Inst. Min. Metall., 147: 1–22.

Corbett, K.D., 1981. Stratigraphy and mineralisation in the Mt Read Volcanics, western Tasmania. Econ. Geol., 76: 209–230.

Corbett, K.D., 1986. Geological setting of mineralisation in the Mt Read Volcanics. In: R.R. Large (Editor), The Mt Read Volcanics and Associated Ore Deposits. Geological Society of Australia, Tasmanian Division, Hobart, pp. 1–10.

Corbett, K.D. and Solomon, M., 1989. Cambrian Mt Read Volcanics and associated mineral deposits. In: C.F. Burrett and E.L. Martin (Editors), Geology and Mineral Resources of Tasmania. Geol. Soc. Aust. Spec. Publ., 15: 84–153.

Cox, S.F., 1981. The stratigraphy and structural setting of the Mt Lyell volcanic-hosted sulphide deposits. Econ. Geol., 76: 231–245.

Edwards, A.B., 1939, Some observations on the mineral composition of the Mt Lyell copper ores, Tasmania and the modes of occurrence. Proc. Australas. Inst. Min. Metall., 114: 67–109.

Eldridge, C.S., Compston, W., Williams, I.S. and Walshe, J.L., 1989. Sulphur isotopic analysis on the SHRIMP Ion Microprobe. In: W.C. Shanks and R.E. Criss (Editors), New Frontiers in Stable Isotope Research: Laser Probes, Ion Probes and Small-sample Analysis. U.S. Geol. Surv. Bull., 1890: 163–174.

Fleet, M.E., MacLean, P.J. and Barbier, J., 1988. Oscillatory-zoned As-bearing pyrite from strata-bound and stratiform gold deposits: an indicator of ore fluid evolution. Econ. Geol. Monogr., 6: 356–362.

Fleischer, M., 1955. Minor elements in some sulphide minerals. In: A.M. Bateman (Editor), Economic Geology, Fiftieth Anniversary Volume. Economic Geology Publishing Co., Urbana, pp. 970–1024.

Green, G.R., 1971. Geology and mineralisation of the Cape Horn-Lyell Comstock area, Mt Lyell. Unpublished B.Sc. (Hons.) Thesis, University of Tasmania.

Green, G.R., Solomon, M. and Walshe, J.L., 1981. The formation of the volcanic-hosted massive sulphide ore deposit at Rosebery, Tasmania. Econ. Geol., 76: 304–338.

Gregory, J.W., 1905. The Mt Lyell mining field, Tasmania. Trans. Australas. Inst. Min. Eng., 10: 26–196.

Gulson, B.L. and Porritt, P.M., 1987. Base metal exploration of the Mt Read Volcanics, western Tasmania: Part II. Lead isotope signatures and genetic implications. Econ. Geol., 82: 291–307.

Hall, G. and Solomon, M., 1962. Metallic mineral deposits. J. Geol. Soc. Aust., 9: 285–309.

Hawley, J.E. and Nichol, I., 1961. Trace elements in pyrite, pyrrhotite and chalcopyrite of different ores. Econ. Geol., 56: 467–487.

Hendry, D.A.F., 1972. The geochemistry of the Mt Lyell copper ores, Tasmania. Unpublished Ph.D. Thesis, University of Cambridge.

Hendry, D.A.F., 1981. Chlorites, phengites and siderites from the Prince Lyell ore deposit, Tasmania and the origin of the deposit. Econ. Geol., 76: 285–303.

Hills, C.L., 1927. A synopsis of the geology of the Lyell district of Tasmania. Proc. Australas. Inst. Min. Metall., 66: 129–148.

Hills, P.B., 1990. The Mount Lyell copper–gold–silver deposits. In: F. Hughes (Editor), Geology of the Mineral Deposits of Australia and Papua New Guinea. Australas. Inst. Min. Metall. Monogr., 14: 1257–1266.

Ineson, P.R., 1989. Introduction to Practical Ore Microscopy. Longman, Earth Science Series, London, 181 pp.

Itoh, S., 1973. Distribution of cobalt in pyrites from some cupiferous pyrite deposits, with special reference to its relationship to metamorphic grade. Bull. Geol. Surv. Jpn., 24: 285–310.

Jago, J.B., Cooper, J.A. and Corbett, K.D., 1977. First evidence for Ordovician igneous activity in the Dial Range Trough, Tasmania. J. Geol. Soc. Aust., 24: 81–86.

Jago, J.B., Reid, K.O., Quilty, P.G., Green, G.R. and Daly, B. 1972. Fossiliferous Cambrian limestone from within the Mt Read Volcanics, Mt Lyell mine area, Tasmania. J. Geol. Soc. Aust., 19: 379–382.

Klemm, D.D., 1962. Untersuchungen über die Mischkristall bildung im Dreieck diagramm FeS_2–CoS_2–NiS_2 und ihre Beziehungen zum Aufbau der naturlichen "Bravoite" (German with English abstract). Neues Jahrb. Mineral. Monatsh., 76–91.

Loftus-Hills, G., 1968. Cobalt, nickel and selenium in Tasmanian ore minerals. Unpublished Ph.D. Thesis, University of Tasmania.

Loftus-Hills, G. and Solomon, M., 1967. Cobalt, nickel and selenium in sulphides as indicators of ore genesis. Miner. Deposita, 2: 228–242.

Markham, N.L., 1968. Some genetic aspects of the Mt Lyell mineralisation. Miner. Deposita, 3: 199–221.

McDonald, M.J., 1968. Progress report on the geology of the West Lyell orebodies at Mt Lyell, Tasmania. Unpublished report, Mt Lyell Mining and Railway Co. Ltd, Queenstown, Tasmania.

Nye, P.B., Blake, F. and Henderson, Q.J., 1934. Report on the geology of the Mt Lyell mining field. Unpublished report, Tasmanian Department of Mines, Hobart.

Ohmoto, H. and Rye, R.O., 1979. Isotopes of sulphur and carbon. In: H.L. Barnes (Editor), Geochemistry of Hydrothermal Ore Deposits, 2nd edn. Wiley, New York, pp. 509–567.

Patterson, D.J., Ohmoto, H. and Solomon, M., 1981. Geologic setting and genesis of cassiterite-sulphide mineralisation at Renison Bell, western Tasmania. Econ. Geol., 76: 393–438.

Perkins, C. and Walshe, J.L., 1993. Geochronology of the Mount Read Volcanics, Tasmania, Australia. Econ. Geol., 88: 1176–1197.

Ramdohr, P., 1969. The Ore Minerals and Their Intergrowths. 3rd edn. Pergamon Press, Oxford, 1174 pp.

Raymond, O.L., 1992. Geology and mineralisation of the southern Prince Lyell deeps, Queenstown, Tasmania. Unpublished M.Sc. Thesis, University of Tasmania.

Reid, K.O., 1975. Mt Lyell copper deposits. In: C.L. Knight (Editor), Economic geology of Australia and Papua New Guinea, 1. Metals. Australas. Inst. Min. Metall. Monogr., 5: 604–619.

Riley, J.F., 1968. The cobaltiferous pyrite series. Am. Mineral., 53: 293–295.

Robinson, B.W. and Kusakabe, M., 1975. Quantitative preparation of sulphur dioxide, for $^{34}S/^{32}S$ analyses from sulphides by combustion with cuprous oxide. Anal. Chem., 47: 1179–1181.

Sillitoe, R.H., 1984. A reappraisal of the Mt Lyell copper deposits, Tasmania: Implications for exploration. Unpublished report, Gold Fields Exploration Pty Ltd, Queenstown, Tasmania.

Sillitoe, R.H., 1985. Further comments on geology and exploration at Mt Lyell, Tasmania. Unpublished report, Gold Fields Exploration Pty Ltd, Queenstown, Tasmania.

Solomon, M., 1964. The spillite–keratophyre association of west Tasmania and thore deposits at Mt Lyell, Rosebery and Hercules. Unpublished Ph.D. Thesis, University of Tasmania.

Solomon, M., 1967. Fossil gossans at Mount Lyell, Tasmania. Econ. Geol., 62: 757–772.

Solomon, M., 1969. The copper-clay deposits at Mount Lyell, Tasmania. Proc. Australas. Inst. Min. Metall., 230: 39–47.

Solomon, M., 1976. "Volcanic" massive sulphide deposits and their host rocks — a review and explanation. In: K. Wolf (Editor), Handbook of Stratabound and Stratiform Ore Deposits. Elsevier, Amsterdam, pp. 21–54.

Solomon, M. and Carswell, J.T., 1989. Mt Lyell. In: C.F. Burrett and E.L. Martin (Editors), Geology and Mineral Resources of Tasmania. Geol. Soc. Aust. Spec. Publ., 15: 125–132.

Solomon, M. and Elms, R.G., 1965, Copper ore deposits of Mt. Lyell. In: J. McAndrew (Editor), Geology of Australian Ore Deposits. 8th Commonwealth Mining and Metallurgical Congress Publication, Vol., 1, pp. 478–484.

Solomon, M. and Groves, D.I., 1994. The Geology and Origin of Australia's Mineral Deposits. Oxford Monographs on Geology and Geophysics, 24, 951 pp.

Solomon, M., Rafter, T.A. and Jensen, M.L., 1969. Isotope studies on the Rosebery, Mt Farrel and Mt Lyell ores, Tasmania. Miner. Deposita, 4: 172–199.

Solomon, M., Vokes, F.M. and Walshe, J.L., 1987. Chemical remobilisation of volcanic-hosted sulphide deposits at Rosebery and Mt Lyell, Tasmania. Ore Geol. Rev., 2: 173–190.

Solomon, M., Eastoe, C.J., Walshe, J.L. and Green, G.R., 1988. Mineral deposits and sulphur isotope abundances in the Mt Read Volcanics between Que River and Mt Darwin, Tasmania. Econ. Geol., 83: 1307–1328.

Springer, G., Schachner-Korn, D. and Long, J.V.P., 1964. Metastable solid solution reactions in the system FeS_2–CoS_2–NiS_2. Econ. Geol., 59: 475–491.

Wade, M.L. and Solomon, M., 1958. Geology of the Mt Lyell mines, Tasmania. Econ. Geol., 53: 367–416.

Walshe, J.L., 1971. Geology of the southern Mt Lyell field and trace element studies of the pyrite mineralisation. Unpublished B.Sc. (Hons.) Thesis, University of Tasmania.

Walshe, J.L., 1977. The geochemistry of the Mt Lyell copper deposits. Unpublished Ph.D. Thesis, University of Tasmania.

Walshe, J.L. and Solomon, M., 1981. An investigation into the environment of formation of the volcanic-hosted Mt Lyell copper deposits using geology, mineralogy, stable isotopes and a six-component chlorite solid solution model. Econ. Geol., 76: 246–284.

White, N.C., 1975. Cambrian volcanism and mineralisation in south-west Tasmania. Unpublished Ph.D. Thesis, University of Tasmania.